Astronomy & Astrophysics manuscript no. paper˙final
September 4, 2012

TMCalc - A fast code to derive Teff and [Fe/H] for FGK stars⋆

S. G. Sousa[1,2], N. C. Santos[1,3,], and G. Israelian[2,4]

[1] Centro de Astrofísica, Universidade do Porto, Rua das Estrelas, 4150-762 Porto, Portugal
[2] Instituto de Astrofísica de Canarias, 38200 La Laguna, Tenerife, Spain
[3] Departamento de Física e Astronomia, Faculdade de Ciências, Universidade do Porto, Rua do Campo Alegre, 4169-007 Porto, Portugal
[4] Departamento de Astrofisica, Universidade de La Laguna, E-38205 La Laguna, Tenerife, Spain

ABSTRACT

We present a new direct spectroscopic calibration for a fast estimation of the stellar metallicity [Fe/H]. This calibrations was computed using a large sample of 451 solar-type stars for which we have precise spectroscopic parameters derived from high quality spectra. The new [Fe/H] calibration is based on weak Fe I lines, which are expected to be less dependent on surface gravity and microturbulence, and require only a pre-determination of the effective temperature. This temperature can be obtained using a previously presented line-ratio calibration. We also present a simple code that uses the calibrations and procedures presented in these works to obtain both the effective temperature and the [Fe/H] estimate. The code, written in C, is freely available for the community and may be used as an extension of the ARES code. We test these calibrations for 582 independent FGK stars. We show that the code can be used as a precise and fast indicator of the spectroscopic temperature and metallicity for dwarf FKG stars with effective temperatures ranging from 4500 K to 6500 K and with [Fe/H] ranging from -0.8 dex to 0.4 dex.

Key words. Stars: fundamental parameters - Stars: abundances - Stars: statistics - Methods: data analysis

1. Introduction

The derivation of stellar parameters is of extreme importance for several fields of astrophysics. Our knowledge of the fundamental parameters of stars, such as the mass and radius, depends directly on the precision that we can achieve when measuring the stellar atmosphere parameters. Parameters that we can directly derive from observations include the effective temperature, surface gravity, and metallicity.

The two major techniques that are normally used to determine these stellar parameters are photometry and spectroscopy. There are many calibrations to help us determine parameters based on the first technique. The IRFM method is one of these methods, that nowadays, is very commonly used because of its reliability in determining the effective temperature of a wide range of stellar types (Blackwell & Shallis, 1977; Blackwell et al., 1979, 1980; Bell & Gustafsson, 1989; González Hernández & Bonifacio, 2009; Ramírez & Meléndez, 2005; Alonso et al., 1996; Casagrande et al., 2006, 2010). Other parameters such as the metal content can also be derived from photometric calibrations (Nordström et al., 2004; Schuster & Nissen, 1989). These parameters can then be used to derive more fundamental parameters, such as mass and radius using calibrations similar to those described in Torres et al. (2010).

The determination of the spectroscopic parameters is not straightforward. A careful analysis is necessary for each stellar spectrum. This can be very time-consuming if you need precise parameters and chemical abundances for several elements. One of the most difficult aspects of a spectroscopic analysis is, undoubtably, the continuum determination. It can be very difficult to derive correct position of the continuum, especially when dealing with poor quality spectra (considering data of low signal-to-noise (S/N) and/or low spectral resolution). Moreover, this difficulty in determining the continuum position also depends on the spectral type of a star. This is because cooler stars tend to have more spectral lines, increasing the amount of blending and leading to the "dilution" of the true continuum. The same happens for different wavelength regions of a given stellar spectrum where the line density strongly increases as you move to shorter wavelengths. This problem can be strongly reduced using automatic tools that are consistent in determining the continuum position, eliminating the errors/offsets, caused by a subjective determination, that are present when using interactive tools.

Another problem that has an important impact on the derivation of spectroscopic stellar parameters is the selection of the lines and their respective atomic parameters. There are two typical choices made by spectroscopists. On the one hand, one can choose to use for each line the atomic parameters defined by a laboratory analysis. This method can have errors as large as 10-20 %. On the other hand, one can adopt new atomic-parameter values determined based on the observed lines in the spectra of a reference star (typically the Sun) and then assume its "well" known spectroscopic parameters. This second option allows us to perform a differential analyses using another star as a reference, and, therefore, when the Sun is used as a standard candle, it is very suitable for solar-type stars (FGK). However, the method becomes imprecise for sufficiently cool and hot stars.

This second option, which is usually referred to in the literature as a differential spectroscopic analysis, was combined previously with automatic codes such as ARES (Sousa et al., 2007) applied in our previous studies (Sousa et al., 2008, 2010, 2011). This allowed us to derive in a systematic and homogeneous way spectroscopic stellar parameters for more than 1000 FGK stars.

⋆ Based on observations collected at La Silla Observatory, ESO, Chile, with the HARPS spectrograph at the 3.6-m telescope (072.C-0488(E)). The code is available for download at www.astro.up.pt/~sousasag/TMCalc

These were then used to derive abundances for a large number of elements (Neves et al., 2009; Adibekyan et al., 2011). In all these works, the derived stellar parameters were proven to be compatible with others derived in different works using a range of independent methods.

In this work, we make use once again of the data of 451 stars presented in Sousa et al. (2008), which consist of very-high quality spectra of both high resolution and high S/N, to perform a new direct spectroscopic calibration of the stellar metallicity [Fe/H]. The calibration is based on weak Fe I lines that depend mainly on temperature and iron abundance and are less dependent on other parameters such as the surface gravity and microturbulence. Therefore, it only requires a pre-determination of the effective temperature. For the determination of the temperature, we can use the line-ratio calibration presented in Sousa et al. (2010) and combine both calibrations to build a simple and fast code that allows a precise estimation of both the effective temperature and [Fe/H].

In Section 2 we recall and discuss the main features of the line-ratio calibration code, presenting some tests done in previous studies to demonstrate its consistency in the particular parameter space of the calibration. In Section 3, we define the new [Fe/H] spectroscopic calibration and explain how we derive it. We also present a simple procedure to derive the final value of [Fe/H] obtained from all the individual line calibrations. In Section 4, we show some simple tests performed on both the calibration sample and an independent large sample of solar-type stars. In the final Section 5, we summarize this work.

2. Temperature based on a line-ratio calibration

The code presented in this work is inspired by a previously published effective-temperature calibration based on line ratios of several spectral lines of different elements (Sousa et al., 2010). This calibration was presented as an excellent tool for determining automatically and quickly a spectroscopic effective temperature, and can be easily used to confirm a spectroscopic temperature determined using the "standard" procedures (see also Gray & Johanson, 1991; Gray, 1994; Gray & Brown, 2001; Gray, 2004; Kovtyukh et al., 2003). This was presented as a possible extension of the ARES code, which can automatically measure the equivalent widths (EWs) of weak absorption spectral lines (Sousa et al., 2007). Desidera et al. (2011) showed that this line-ratio calibration can return good estimates of the temperature, even for solar-type stars up to relatively high rotation rates (up to 18 Km/s). This excedes the abilities of typical EW methods owing to the increase in the number of blends with higher rotation of the stars.

In Figure 1, we compare the temperatures derived with the line-ratio calibration of Sousa et al. (2010) with those derived using the standard spectroscopic procedure (Sousa et al., 2008, 2011). The top plot shows this comparison for the sample of stars used to calibrate the line ratios. As expected, the consistency is very good. This plot is important to illustrating the typical dispersion that we obtain using the line-ratio calibration.

In the bottom plot of the same figure, we show the same comparison for an "independent" sample of stars (independent in the sense that these stars were not used to compute the calibration of each line ratio). It is clear that the comparison is also consistent. Both plots were presented in previous works, and they are presented here to recall that the temperature inferred from the line ratio is consistent with our standard spectroscopic method, within the ranges defined for the calibration. Therefore, we can use the line-ratio calibration in order to determine the temperature of a star, and then examine the strength of the iron absorption-lines and quickly find a calibration of [Fe/H].

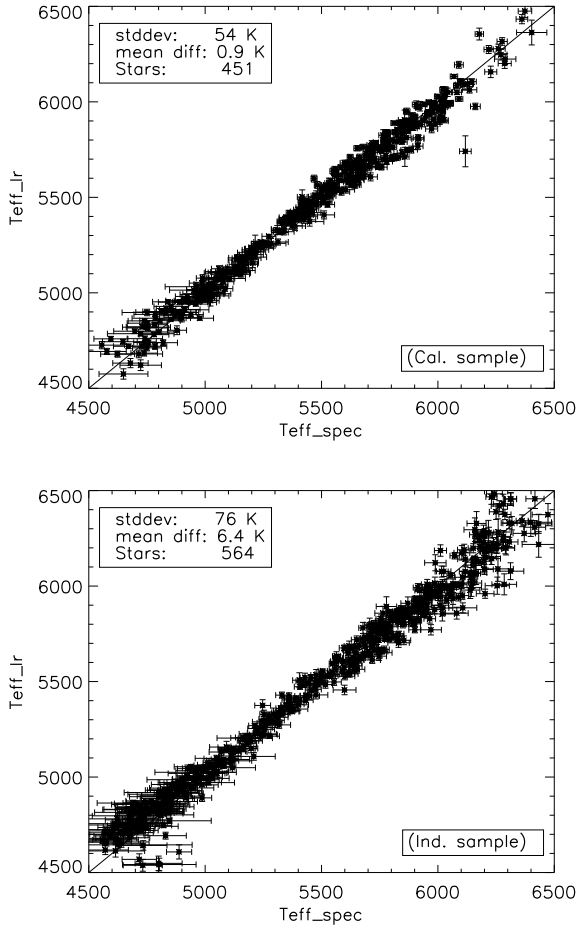

Fig. 1. In the top panel, we show the comparison between the effective temperatures derived from our standard spectroscopy analysis and the ones derived using the line-ratio code for the sample used to derive the calibration (labelled Cal. Sample in the plot adapted from Sousa et al. (2010)). In the bottom plot, we show a similar plot but this time for the sample of stars presented in Sousa et al. (2011). This corresponds to a sample that is independent of the derived calibration. In both panels, we present the mean difference and the standard deviation for the comparisons.

3. [Fe/H] calibration

3.1. Selection of lines

To obtain a calibration that help us determine [Fe/H], we need to compile a list of iron lines that are observed for solar-type stars. For this step, we started with the "stable" line-list presented in Sousa et al. (2008), which is a list of iron lines chosen to ensure that they are appropriate for an automatic determination of EWs with ARES. The next step was to select lines that should be independent of both surface gravity and microturbulence. In other words we needed at this point, to select lines that depend mostly on temperature and [Fe/H].

We can easily ensure the independence of the calibration of the surface gravity by selecting only the iron lines that corresponds to the neutral state (Fe I). This is because the ionized iron lines (e.g. Fe II) depend strongly on the surface gravity, in

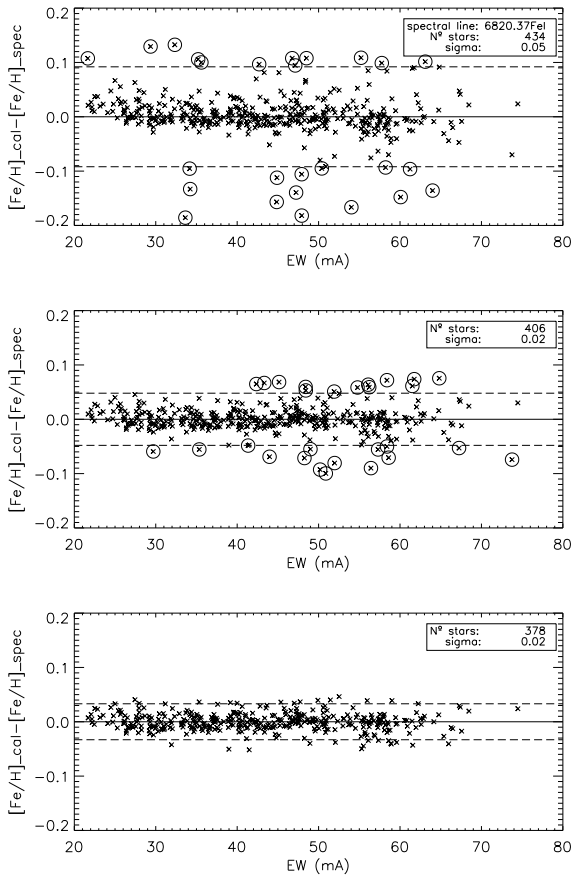

Fig. 2. The sequence of plot from top to bottom shows the removal of outliers for the iron line at 6820.37 Å.

contrast to the neutral iron lines (Gray, 1992). We therefore take out all the Fe II lines from the original list.

Finally, the microturbulence parameter may have a strong impact on the strength of a spectral line, particulary for stronger lines. Weak lines are known to be reasonably independent of microturbulence.

One problem that we face in defining our linelist is that the strength of each individual line depends strongly on the effective temperature and [Fe/H]. We can therefore only eliminate a line after its line strengh has been measured and checked to be in the regime where it is independent of microturbulence. Therefore, for this work we consider our cut at 75 mÅ. This value seems to be reasonable taking into account not only the microturbulence dependence, but also considering that lower values will strongly reduce the number of lines acceptable for the calibrations.

We also wish to note that there is a known dependence of the microturbulence on the temperature (e.g. Pilachowski et al., 1996; For & Sneden, 2010). Therefore, the microturbulence dependence seen for the stronger lines may be removed significantly by the temperature fitting in our calibrations. Together with the restrictions that we impose on the line selection we can strongly eliminate any microturbulance dependence from our calibrations.

3.2. The [Fe/H] calibration

To derive the calibration for [Fe/H], we again used the sample of stars presented before for the temperature line-ratio calibration. This sample is composed of 451 solar-type stars that were all observed with HARPS to obtain high-resolution spectra (R ∼ 110000). These stars were part of the HARPS survey for extra-solar planets (Mayor et al., 2011). The S/N for this sample varies from 70 to 2000, with 90% of the spectra having a S/N higher than 200. It is a very well-established sample with homogeneous spectroscopic parameters that have been compared with other independent methods.

To ensure consistency with the previous line-ratio calibration, we used the same EW measurements.

For each line, a calibration was computed following the equation:

$$\begin{aligned} EW =& C_0 + C_1 * [Fe/H] + C_2 * T_{eff} + \\ & C_3 * [Fe/H]^2 + C_4 * T_{eff}^2 + \\ & C_5 * [Fe/H] * T_{eff}. \end{aligned} \quad (1)$$

We choose to use this equation in order to have an easy (and quickly attainable) representation of the physical dependence between the line strength, the effective temperature, and the iron abundance. To extract the iron abundance from this equation, we perform a simple invertion of $[Fe/H]$.

In Fig. 2, we show the results of an iterative process for the determination of the calibration coefficients for the iron line at 6820.37 Å. In this process, we first select the lines (stars) accordingly to the discussion in Sect. 3.1, i.e. removing all points whith EWs larger than 75 mÅ (each point is the EW for a star in the sample). At this step, we also choose to remove the lines with EWs smaller than 20 mÅ. This is because for these small lines we have a larger relative error in the EW. We then fit the remaining points with the equation and perform the first outlier removal, choosing a 2 σ threshold. We repeat the process one more time to eliminate extra outliers. These outliers are mainly due to poor automatic EW measurements that are typically related to either a bad continuum determination or strongly blended lines. The final fitted coefficients are kept, together with the final number of stars used, the slope of the direct comparison between the calibrated and the spectroscopic [Fe/H], and the respective standard deviation of the fit.

This procedure was performed for all the lines in the initial iron line-list. Finally, we made a careful selection of the lines, considering the results of each individual fit. This selection was performed to ensure that each calibration satisfies the following conditions:

1. The direct comparison between the calibrated and the spectroscopic [Fe/H] has a slope within 3% of the identity line.
2. The standard deviation of the individual line calibration is less than 0.04 dex.

The values used in these two conditions were chosen to keep a significantly large number of lines in order to increase the statistical meaning of the final metallicity derivation. In this case we want to note we choose not to neglect lines that have a given minimum of the final number of stars used for the individual fit. The reason for this is that we remove lines of the fit accordingly to their strength, which means that depending on the temperature and metallicity of a star, a given line will be either stronger or weaker in specific space regions of these two parameters. Therefore, the only concern that we have in these cases is to ensure that we take into account that each individual calibration is only valid within each individual parameter space.

Table 2 lists a sample of the total of 149 lines that have passed this process and can be used for our [Fe/H] determination. The full table is available in its electronic format.

3.3. [Fe/H] estimation from the line calibrations

From the calibrated lines, we can now derive a final value for the global [Fe/H] for a given star. The procedure that we propose here is the same as that presented for the temperature determination based on line ratios (Sousa et al., 2010). We summarize this procedure in the following items:

- First we compute the [Fe/H] determination using each calibrated line from Table 2.
- Secondly, we select the calibrated lines accordingly to the limits of each individual calibration. In this step, we choose to increase the limits by 100K in both directions. The errors coming from the temperature line-ratio calibration are of this order of magnitude and therefore we wish to guarantee that we do not remove lines that can give a reasonable estimation of [Fe/H].
- Finally, we compute the weighted average of the [Fe/H] results, considering the standard deviation of each individual calibration.

This procedure is repeated twice with a 2 σ outlier removal, eliminating in this process the EWs that were not (for any reason) performed correctly.

3.4. Errors

The easiest error estimate that we can extract from our procedure is to assume the dispersion in the values given by all the individual calibrations. If one considers that each individual calibration is independent of all the others, we can divide the dispersion by the square root of the final number of individual calibrations used.

It is wise, however, to include the error in the temperature. To do this, we choose to use a straightforward estimation of this error, which is to derive the error in [Fe/H] using the limits given by the temperature error (1-σ). The final error is obtained by evaluating the quadratic sum of the two sources of errors.

3.5. Using TMCalc to estimate temperature and [Fe/H] for solar-type stars

The calibration presented here is only useful when you have a temperature estimation. We therefore developed a free code, implemented in C language, that combines both the line ratio calibration and the [Fe/H] calibration presented here. The code is available online at the ARES web page[1]. The code comes with a simple shell script "TMCalc", which can be used as the driver to run the C code with an easy shell-command line. This makes the code ready to be included in any kind of a spectral analysis pipeline. The only requirement is to have the spectrum (e.g. coming from the pipeline) in a format ready to be used with ARES.

4. Testing the code

4.1. The calibration sample

Figure 3 shows the results obtained when applying the code to the calibration sample. Here we compare the calibrated [Fe/H] against the spectroscopic [Fe/H]. The result is consistent, thus can be expected since in this case the sample is the same as that used to compute the line calibrations.

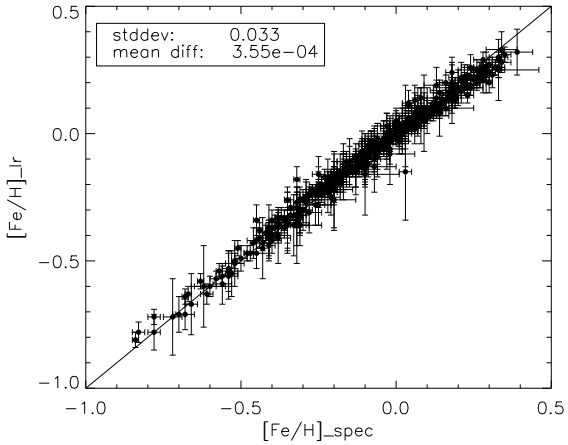

Fig. 3. Direct comparison between the calibrated [Fe/H] and the spectroscopic [Fe/H] for the sample used to compute the calibrations.

In Fig. 4, we try to identify any dependences of the value of [Fe/H] derived from the calibration on other spectroscopic parameters such as temperature, surface gravity, and spectroscopic [Fe/H]. It is possible to see from this figure the ranges of spectroscopic parameters for which this calibration is valid. It is clear that these come directly from the star properties in the sample, which is typically composed of solar-type stars with effective temperatures ranging between 4556 K and 6403 K, and with surface gravities typical of dwarf stars and a few sub-giants ([3.68, 4.62]). All these stars have metallicities of around solar, ranging from -0.84 dex to 0.39 dex.

It is clear from Fig. 4 that there is no clear trend, except for the spectroscopic [Fe/H] itself. An offset is clearly visible for the metal-rich stars, but the maximum differences remain within 0.1 dex, which can nevertheless be significant. This offset is a result of some extra dependence that the individual line calibrations were unable to extract, or is merely an artifact of the fit, since the offset is only observed in the upper limit to [Fe/H]. Instead of applying a higher order polynomial for each individual calibration and trying to eliminate this offset, we choose to perform a simpler and more direct correction. From the figure, we can see that we can fit the points with a simple horizontal line for [Fe/H] < -0.2 (dashed line). This corresponds to a calibrated [Fe/H] ~ -0.187, given that the horizontal line has a value of ~ 0.013. For higher [Fe/H] values, we use a second-order polynomial to consistently fit the offset (dashed-point line). We therefore use the following equations to perform the correction for the calibrated [Fe/H] in these two regimes:

$$\begin{aligned}[Fe/H]_{cor} =& [Fe/H]_{cal} - (0.013) \\ & \text{if } ([Fe/H]_{cal} < (-0.187)), \\ \\ [Fe/H]_{cor} =& [Fe/H]_{cal} - (-0.000726960 \\ & - 0.0950966 * [Fe/H]_{cal} \\ & - 0.128329 * [Fe/H]^2_{cal} \\ & \text{if } ([Fe/H]_{cal} \geq (-0.187)).\end{aligned} \quad (2)$$

[1] http://www.astro.up.pt/~sousasag/ares)

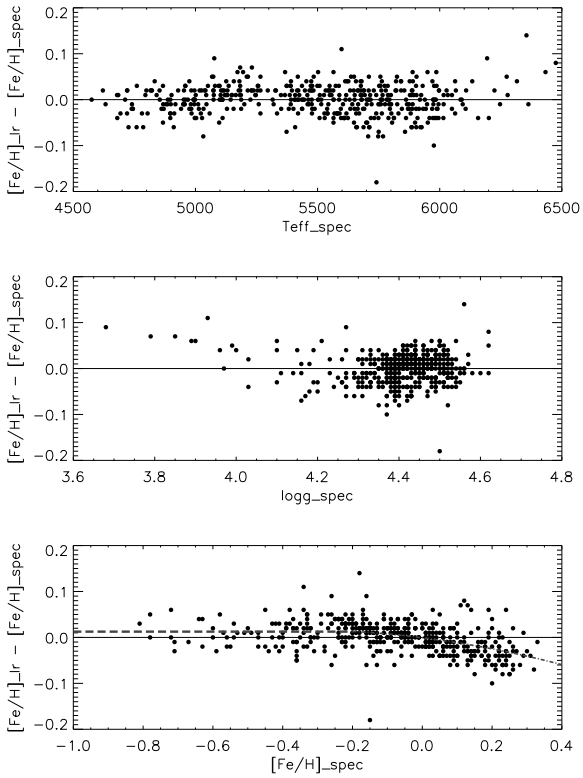

Fig. 4. Difference between the calibrated [Fe/H] and the spectroscopic [Fe/H] and its dependence on the other spectroscopic stellar parameters such as the effective temperature (top panel), the surface gravity (middle panel), and the spectroscopic [Fe/H] (bottom panel). The dashed and dashed pointed lines are fits to the date described in detail in the text.

This equation is applied at the end of the procedure to correct the offset that can be seen in Figure 4.

In Figure 5, we show the effect of the correction for the sample used for the calibration. The dispersion in slightly smaller and the offset is close to zero as expected. However, this is still the sample of stars used to derive the calibration, hence the consistency of this result is expected. What is interesting to show at this stage is the "small" dispersion in the evaluated [Fe/H], which is typically around ~ 0.03 dex. This value can be used as a reference to indicate the quality of the final corrected calibration.

4.2. Constrains on line strenghts

As discussed before, we choose lines of a specific range of strengths: weak lines in order to avoid any dependence on the microturbulence, but not those that are weak to avoid the intrinsic errors in the measurements of very weak lines. The reader may be concerned about these restrictions and the possible systematics that they can produce on the described calibrations. For instance, for low temperature stars, these restrictions will tend to eliminate the stronger lines in the metal-rich stars, while in hotter stars, different lines (that are weaker) will be eliminated for the metal-poor stars owing to the poorer constraints. Even without our poorer constraints, the iron lines tend to disappear from the spectrum in these cases, since they are metal-poor. Therefore, for different types of stars, we use different sets of lines, which could introduce systematic errors into the calibrations.

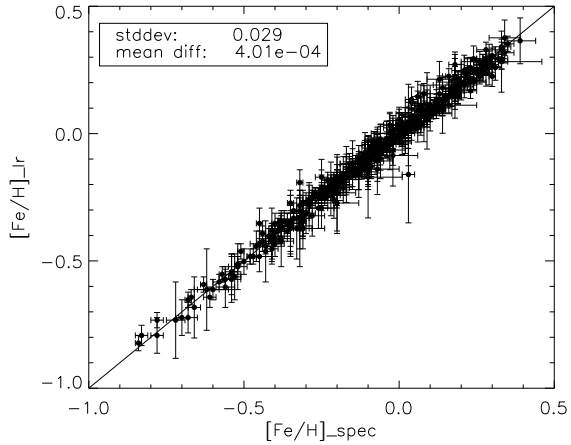

Fig. 5. Direct comparison between the corrected calibrated [Fe/H] and the spectroscopic [Fe/H] for the sample used to compute the calibrations.

Figure 6 tries to identify any of the described possible systematic errors. In the top panels of this figure, we show the same kind of direct comparison between the corrected calibrated [Fe/H] and the spectroscopic [Fe/H], but divide the sample into different temperature regimes. On the left we see the lower temperature stars (T_{eff} < 5000 K), and on the right the hotter stars (T_{eff} > 5800 K). The comparisons remains consistent with a small dispersion and no visible trend for the different temperature regimes. In the bottom panels, we present the number of individual calibrations used in each star. In these plots the decrease in the number of lines used is clear for the metal-poor stars in both temperature regimes. For the cooler stars, the reduction in the number of lines is also clear for the more metallic stars. This is the effect that we described before and is a result of neglecting the stronger lines to eliminate the microturbulence dependence. Although the number of lines is smaller owing to the discussed systematics, it is clear from the comparison that the results are consistent, and the selection of the lines using the indicated constraints on the line strength seem to produce good results.

4.3. Large independent sample for direct comparison

We only showed the test on a very well-defined sample, composed of stars with data of high resolution and high S/N, which was used to define the calibration. At this point, we wish to show an independent test, in the sense that we use a different sample of stars that was not used to compute the calibration. This "independent" sample is composed of a total of 582 FGK stars for which the parameters were determined using the same homogeneous spectroscopic method. The details of these determinations can be seen in Sousa et al. (2011). The main difference regards the spectral quality of this sample: this sample typically has a lower S/N than the calibration sample. 75% of the stars have S/N lower than 200, while 90% of the stars in the calibration sample have data of S/N higher than 200.

In Figure 7, we compare the standard spectroscopic derivation result with the calibration presented here for this "independent" large sample of stars.

The result of this direct comparison is very good. The mean difference is close to zero, indicating that there is no clear offset in the determined [Fe/H]. However, the dispersion (~0.04 dex)

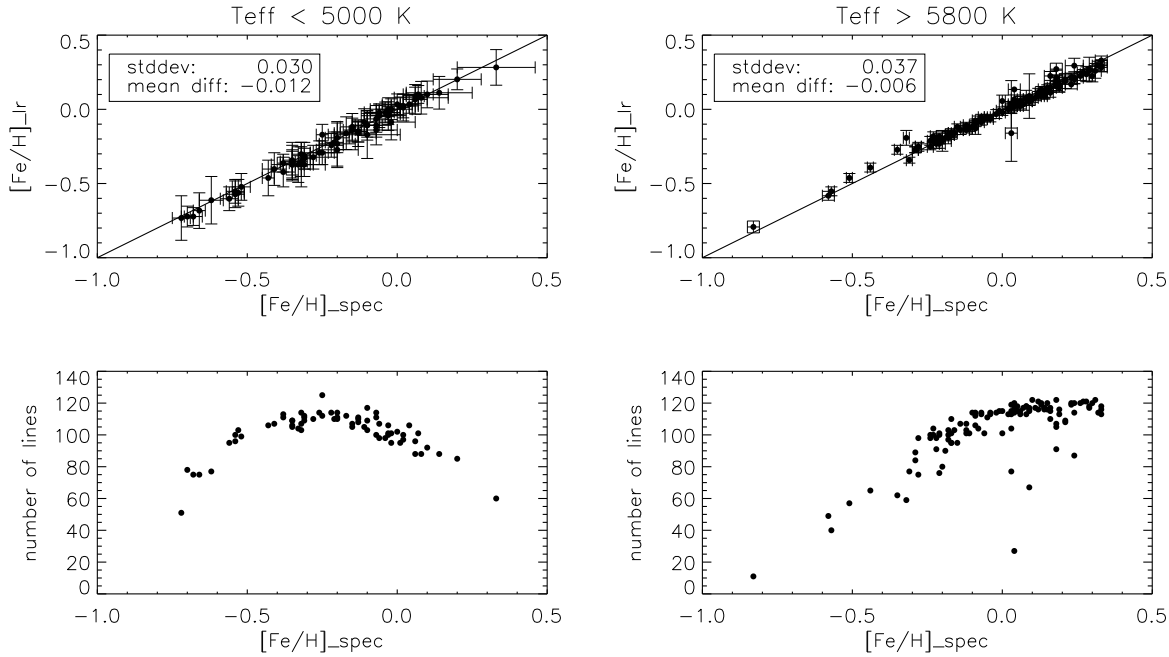

Fig. 6. Direct comparison between the corrected calibrated [Fe/H] and the spectroscopic [Fe/H] for the sample used to compute the calibrations for two different temperature regimes: cool stars (Top left panel) and hotter stars (top right panel). In the bottom panel, we present the number of individual calibrations used in each star.

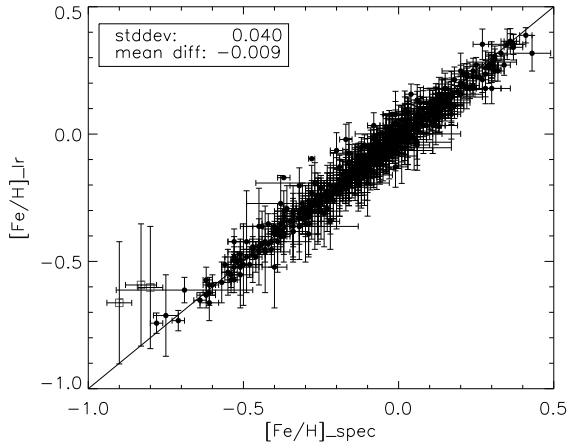

Fig. 7. Direct comparison of the corrected calibrated [Fe/H] and the spectroscopic [Fe/H] for an independent sample of solar-type stars. The three grey squares indicate stars for which the code obtained results outside the calibrated [Fe/H].

is larger than for the previous comparisons. This is expected because this sample has typically a lower S/N. In addition, this large "independent" sample has a few stars that lie outside the limits of the calibration. Amoung the 582 stars that belong to this sample, the code was able to derive values for a total of 556 stars. Amoung these stars, there are still a few that are outside the limits of the calibration. This can be clearly seen in the figure at lower metallicities where we have at least three stars with metallicities lower than -0.8 dex (plotted as grey squares in the Figure). The error bars for these three stars are large compared to those for the rest of the stars. This is due to the far smaller number of iron lines (about ten) used in the estimation of the calibrated [Fe/H]. The number of lines and their respective errors derived from the procedure previously described can be used to reliably check whether the star is within the limits of the parameter space of the calibration.

After this has been noted, the remaining results are very consistent and reveal that this calibration, both in temperature and [Fe/H], is precise enough to be used within its limits, to efficiently derive these two atmosphere parameters, either as a first approximation or as a check of other standard spectroscopic determinations.

4.4. Spectral resolution and S/N

To evaluate how this procedure works for different spectral resolutions and different values of S/N, we computed several solar spectra, first with different levels of S/N and then with different levels of resolution. The original spectrum was obtained using the Kurucz Solar Atlas. The noise was created using a Gaussian distribution and we introduced the artificial instrumental resolution using the "rotin3" routine in SYNSPEC[2] (Hubeny et al., 1994). We first created ten different S/N levels to be included in the original spectrum (10, 25, 50, 75, 100, 150, 200, 300, 400, and 500). We then created ten addicional different spectra with resolutions ranging from 10000 to 100000, corresponding to FWHM of 0.550 Å and 0.055 Å at the central wavelength 5500 Å. For this spectra, we included the noise to simulate spectra with S/N ∼ 200, which more closely represent the real spectra. We generated the spectra in the region [4000 Å - 7000 Å] in order to cover our linelist.

For the spectra of different resolutions, the EW measurements were all performed with ARES using the same input parameters (smoothder=4, space=3, rejt=0.994, lineresol=0.07), except for the spectrum with the lowest resolution for which we adapted a "smoothder" parameter of 12. For the different S/N

[2] http://tlusty.gsfc.nasa.gov/index.html

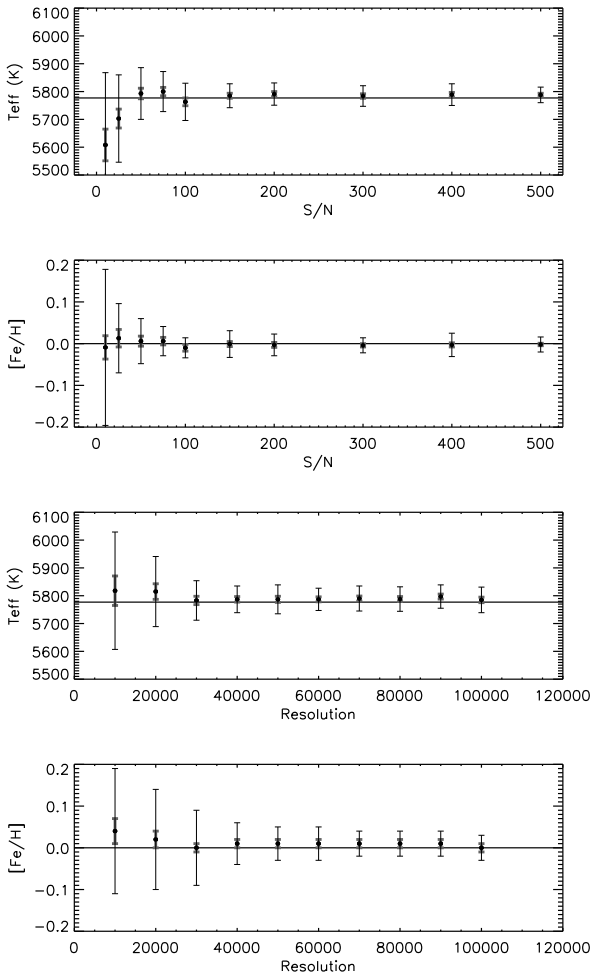

Fig. 8. Temperature and [Fe/H] determined using our calibrations for the simulated solar spectrum with different sets of resolutions and S/N. We show two different error estimations, the thin black error bars representing only the dispersion in the individual calibrations, and the thick grey error bar where we also take into account the number of individual calibrations used. See text for details.

spectra, the ARES parameter "rejt" changed accordingly to the S/N of the spectra, using the recommended values discussed in Sousa et al. (2011). The results can be seen in Figure 8. The two top panels shows the results for the solar spectra of different S/N, the two bottom plots for the solar spectra of different resolution. We also present two of the errors estimations given by the code. The smaller and thicker grey error-bars represent the errors obtained by considering the dispersion in the individual calibration and the number of independent lines used. The thin black error bars presented in this figure are the ones obtained using only the dispersion in the individual calibrations, ignoring the number of calibrations used. The results are consistent even for the lower resolutions, where the strong increase in the errors originating directly from dispersion in the independent calibrations can be clearly seen. This proves that the calibrations presented in this work can be safely used for lower resolution spectra. In terms of the S/N, the results are also quite consistent down to S/N ∼ 25. For this low S/N, the temperature estimation starts to deviate from the expected one, although the errors are large and greater than the offset. We note that for the [Fe/H] even for very low S/N spectra the values are very close to the expected [Fe/H]=0.

5. Summary

We have presented a new spectroscopic line calibration to efficiently estimate the stellar [Fe/H]. This calibration depends on both the temperature and the strength of the iron lines. We make available a free code that combined with ARES and a previous temperature line-ratio calibration allows us to estimate both the spectroscopic stellar effective-temperature and the [Fe/H]. We tested this code with a large sample of solar-type stars and confirmed that these calibrations are consistent within the parameter space defined for the calibrations. This code can easily be applied to a spectroscopic data-analysis pipeline in order to quickly obtain precise estimations of these important spectroscopic parameters.

These calibrations should not replace the more precise standard spectroscopic analyses that are typically more time-consuming. These standard methods should definitely be used if one whishes to study stars individually. However, the tool that we present in this work can be very useful for determining precise parameters for large amounts of data. Typical examples are the data sets of spectroscopic surveys, which are very large and for which people normally search for statistical trends among the propreties of the many survey targets.

Acknowledgements. S.G.S acknowledges the support from the Fundação para a Ciência e Tecnologia (Portugal) in the form of a grants SFRH/BPD/47611/2008. NCS thanks for the support by the European Research Council/European Community under the FP7 through a Starting Grant. We also acknowledge support from FCT and FSE/POPH in the form of grants reference PTDC/CTE-AST/098528/2008, PTDC/CTE-AST/098754/2008, and PTDC/CTE-AST/098604/2008.

References

Adibekyan, V. Z., Santos, N. C., Sousa, S. G., & Israelian, G. 2011, A&A, 535, L11
Alonso, A., Arribas, S., & Martinez-Roger, C. 1996, A&AS, 117, 227
Bell, R. A. & Gustafsson, B. 1989, MNRAS, 236, 653
Blackwell, D. E., Petford, A. D., & Shallis, M. J. 1980, A&A, 82, 249
Blackwell, D. E. & Shallis, M. J. 1977, MNRAS, 180, 177
Blackwell, D. E., Shallis, M. J., & Selby, M. J. 1979, MNRAS, 188, 847
Casagrande, L., Portinari, L., & Flynn, C. 2006, MNRAS, 373, 13
Casagrande, L., Ramírez, I., Meléndez, J., Bessell, M., & Asplund, M. 2010, A&A, 512, A54+
Desidera, S., Covino, E., Messina, S., et al. 2011, A&A, 529, A54+
For, B.-Q. & Sneden, C. 2010, AJ, 140, 1694
González Hernández, J. I. & Bonifacio, P. 2009, A&A, 497, 497
Gray, D. F. 1992, The observation and analysis of stellar photospheres., ed. Gray, D. F.
Gray, D. F. 1994, PASP, 106, 1248
Gray, D. F. 2004, Advances in Space Research, 34, 308
Gray, D. F. & Brown, K. 2001, PASP, 113, 723
Gray, D. F. & Johanson, H. L. 1991, PASP, 103, 439
Hubeny, I., Lanz, T., & Jeffery, C. 1994, TLUSTY & SYNSPEC - A user's guide
Kovtyukh, V. V., Soubiran, C., Belik, S. I., & Gorlova, N. I. 2003, A&A, 411, 559
Mayor, M., Marmier, M., Lovis, C., et al. 2011, ArXiv e-prints
Neves, V., Santos, N. C., Sousa, S. G., Correia, A. C. M., & Israelian, G. 2009, A&A, 497, 563
Nordström, B., Mayor, M., Andersen, J., et al. 2004, A&A, 418, 989
Pilachowski, C. A., Sneden, C., & Kraft, R. P. 1996, AJ, 111, 1689
Ramírez, I. & Meléndez, J. 2005, ApJ, 626, 446
Schuster, W. J. & Nissen, P. E. 1989, A&A, 221, 65
Sousa, S. G., Alapini, A., Israelian, G., & Santos, N. C. 2010, A&A, 512, A13+
Sousa, S. G., Santos, N. C., Israelian, G., et al. 2011, A&A, 526, A99+
Sousa, S. G., Santos, N. C., Israelian, G., Mayor, M., & Monteiro, M. J. P. F. G. 2007, A&A, 469, 783
Sousa, S. G., Santos, N. C., Mayor, M., et al. 2008, A&A, 487, 373
Torres, G., Andersen, J., & Giménez, A. 2010, A&A Rev., 18, 67

Table 2. [Fe/H] line calibration table

id	*stddev*	*ns*	λ	c_0	c_1	c_2	c_3	c_4	c_5	T_{eff}^{min}	T_{eff}^{max}	*fehmin*	*fehmax* †
1	0.038	296	6842.04	-2.648e+02	1.116e+01	1.196e-01	1.559e+01	-1.201e-05	5.558e-03	4578	6276	-0.45	0.39
2	0.015	386	4523.40	3.340e+01	9.804e+00	3.054e-02	-6.349e-01	-4.963e-06	6.433e-03	4624	6403	-0.78	0.39
3	0.022	227	4537.67	2.850e+02	1.119e+02	-7.090e-02	1.515e+01	4.253e-06	-1.374e-02	4578	6026	-0.72	0.39
4	0.014	322	4551.65	-7.152e+01	3.406e+01	5.782e-02	5.992e+00	-7.036e-06	1.309e-03	4624	6287	-0.66	0.39
5	0.030	339	4554.46	8.308e+02	1.017e+02	-2.340e-01	-5.797e+00	1.677e-05	-1.028e-02	4649	6403	-0.72	0.39
6	0.032	362	4561.41	2.503e+01	9.022e+01	2.946e-02	1.166e+01	-4.717e-06	-6.692e-03	4556	6374	-0.72	0.39
7	0.015	396	4566.52	2.469e+01	4.034e+01	3.551e-02	6.998e+00	-5.498e-06	1.472e-03	4624	6374	-0.78	0.39
8	0.037	399	4574.22	1.069e+02	1.187e+02	1.120e-02	1.076e+01	-3.925e-06	-1.193e-02	4556	6361	-0.84	0.39
9	0.035	341	4574.72	-1.094e+02	-4.674e+01	8.927e-02	-5.797e+00	-1.049e-05	1.508e-02	4679	6374	-0.84	0.35
10	0.029	326	4579.33	-1.005e+01	2.901e+01	4.280e-02	3.486e+00	-6.285e-06	2.275e-03	4578	6276	-0.72	0.35
11	0.018	348	4593.53	-1.559e+02	4.349e+01	8.990e-02	1.158e+01	-1.002e-05	1.026e-04	4578	6287	-0.66	0.39
12	0.016	377	4596.41	-6.229e+01	4.851e+01	6.032e-02	1.230e+01	-7.593e-06	-2.193e-04	4624	6361	-0.72	0.39
13	0.029	168	4602.00	1.424e+02	-6.960e+01	-6.436e-04	-9.508e+00	-2.015e-06	1.797e-02	5023	6361	-0.84	0.30
14	0.020	380	4635.85	-5.750e+01	-4.600e+01	6.402e-02	-7.687e+00	-7.701e-06	1.477e-02	4556	6374	-0.84	0.39
15	0.018	395	4661.54	-1.697e+01	2.606e+01	4.171e-02	3.297e+00	-5.604e-06	3.134e-03	4578	6287	-0.78	0.39
16	0.037	384	4690.14	-1.012e+01	-2.301e+01	4.402e-02	1.871e+00	-5.633e-06	1.152e-02	4556	6403	-0.84	0.35
17	0.021	165	4741.53	1.279e+02	-5.548e+01	3.355e-03	-7.231e+00	-2.223e-06	1.614e-02	5107	6374	-0.83	0.21
18	0.024	365	4749.95	-1.323e+02	2.246e+01	8.116e-02	2.547e+00	-8.989e-06	3.883e-03	4578	6403	-0.72	0.39
19	0.024	356	4757.58	-7.143e+01	-2.808e+01	6.850e-02	-1.834e+00	-8.017e-06	1.250e-02	4578	6374	-0.84	0.35
20	0.024	387	4799.41	-1.553e+02	-3.570e+01	8.893e-02	-4.295e+00	-9.673e-06	1.326e-02	4578	6403	-0.78	0.35
21	0.020	374	4802.88	-9.156e+01	-3.493e+01	7.265e-02	-3.840e+00	-8.020e-06	1.323e-02	4556	6374	-0.84	0.33
22	0.025	331	4808.15	-5.913e+01	-1.793e+01	5.758e-02	3.759e+00	-7.360e-06	1.016e-02	4556	6289	-0.68	0.39
23	0.017	237	4809.94	1.115e+02	6.798e+01	-8.873e-03	1.471e+01	-1.222e-06	-5.567e-03	4556	6161	-0.56	0.39
24	0.028	210	4811.05	5.310e+02	1.336e+02	-1.522e-01	1.884e+01	1.087e-05	-1.721e-02	4556	5917	-0.56	0.39
25	0.018	215	4885.43	2.976e+01	-3.157e+01	3.593e-02	-9.299e+00	-4.990e-06	1.183e-02	4679	6403	-0.84	0.30
26	0.027	385	4952.65	-3.128e+02	-2.876e+00	1.446e-01	4.440e+00	-1.400e-05	1.007e-02	4578	6374	-0.84	0.33
27	0.024	340	4961.92	3.544e+02	8.169e+01	-8.764e-02	1.032e+01	5.360e-06	-6.613e-03	4647	6361	-0.70	0.39
28	0.039	94	4967.90	-6.541e+02	-2.072e+02	2.631e-01	-1.695e+01	-2.356e-05	4.177e-02	4679	6374	-0.84	0.04
29	0.018	249	4993.70	5.145e+02	1.031e+02	-1.158e-01	1.718e+01	6.340e-06	-5.782e-03	4989	6403	-0.84	0.30
30	0.033	394	5054.65	1.340e+02	1.432e+00	-3.989e-03	1.245e+01	-2.134e-06	8.187e-03	4556	6403	-0.68	0.35
31	0.014	156	5109.65	4.803e+02	3.256e+01	-1.157e-01	3.659e-01	7.850e-06	3.189e-03	4999	6374	-0.83	0.18
32	0.019	358	5223.19	5.883e+01	2.439e+01	1.539e-02	4.940e+00	-3.539e-06	3.085e-03	4556	6361	-0.70	0.39
33	0.023	158	5225.53	3.136e+01	-2.554e+01	5.535e-02	-1.776e+00	-8.344e-06	1.168e-02	5023	6403	-0.84	0.30
34	0.032	364	5228.38	-1.692e+02	-3.751e+01	1.017e-01	-8.345e+00	-1.073e-05	1.447e-02	4578	6403	-0.84	0.33
35	0.020	289	5243.78	-4.838e+01	-1.845e+01	6.173e-02	-2.325e+00	-7.368e-06	1.151e-02	4647	6374	-0.84	0.30
36	0.018	186	5247.06	1.322e+02	-2.566e+01	2.116e-02	-2.135e+00	-5.616e-06	1.181e-02	5023	6361	-0.84	0.30
37	0.037	194	5250.21	-2.069e+02	7.157e+00	1.410e-01	3.865e+00	-1.618e-05	6.933e-03	5009	6403	-0.84	0.30
38	0.030	345	5288.53	-1.348e+02	-3.033e+01	8.871e-02	-3.576e+00	-9.581e-06	1.314e-02	4556	6374	-0.84	0.31
39	0.018	355	5295.32	-1.179e+02	2.315e+01	7.142e-02	4.884e+00	-7.923e-06	3.454e-03	4578	6361	-0.56	0.39
40	0.023	137	5376.83	-1.145e+02	2.713e+01	6.600e-02	1.654e+01	-7.583e-06	6.292e-04	4556	5914	-0.35	0.39
41	0.016	334	5379.58	-7.200e+00	-1.588e+00	4.834e-02	-1.483e+00	-6.308e-06	8.373e-03	4624	6374	-0.84	0.33
42	0.025	379	5386.34	-4.134e+00	1.323e+01	3.585e-02	-3.517e-01	-5.080e-06	5.200e-03	4578	6374	-0.72	0.35
43	0.022	229	5395.22	-1.735e+02	5.967e+01	8.896e-02	2.075e+01	-9.590e-06	-4.265e-03	4556	6161	-0.38	0.39
44	0.030	205	5398.28	-2.415e+02	-1.068e+02	1.248e-01	-8.674e+00	-1.222e-05	2.583e-02	4649	6374	-0.84	0.21
45	0.026	375	5406.78	1.048e+02	2.616e+01	-6.547e-04	3.715e+00	-1.954e-06	3.123e-03	4647	6403	-0.78	0.39
46	0.023	363	5417.04	-9.121e+01	3.169e+01	6.766e-02	1.222e+01	-7.924e-06	3.116e-03	4556	6361	-0.68	0.39
47	0.038	211	5432.95	8.162e+01	-5.922e+01	7.810e-03	-4.982e+00	-1.711e-06	1.828e-02	4578	6374	-0.84	0.19
48	0.015	399	5436.30	-9.556e+01	2.742e+01	7.104e-02	6.297e+00	-8.221e-06	3.754e-03	4578	6374	-0.78	0.39
49	0.026	383	5436.59	-3.519e+01	-1.176e+01	6.364e-02	5.610e+00	-8.628e-06	1.091e-02	4556	6374	-0.78	0.39
50	0.025	345	5441.34	3.332e+00	1.252e+02	3.525e-02	1.832e+01	-5.217e-06	-1.337e-02	4671	6374	-0.60	0.39
51	0.033	305	5461.55	4.943e+02	8.377e+01	-1.402e-01	8.728e+00	1.023e-05	-7.197e-03	4723	6361	-0.62	0.39
52	0.019	387	5464.28	-2.130e+02	-2.285e+01	1.091e-01	-1.938e+00	-1.135e-05	1.157e-02	4556	6374	-0.78	0.39
53	0.026	369	5466.99	-8.944e+01	4.082e+01	6.822e-02	1.549e+01	-8.064e-06	1.694e-03	4578	6374	-0.72	0.39
54	0.030	204	5473.17	3.299e+01	7.443e+01	1.203e-02	1.686e+01	-2.516e-06	-7.635e-03	4556	5973	-0.41	0.39
55	0.023	301	5481.25	-1.329e+02	3.132e+01	1.024e-01	-2.019e-01	-1.194e-05	4.071e-03	4698	6287	-0.84	0.33
56	0.023	97	5491.83	-3.001e+02	8.196e+01	1.321e-01	3.658e+01	-1.349e-05	-9.679e-03	4723	5914	-0.11	0.39
57	0.023	384	5522.45	2.861e+01	9.286e+00	2.923e-02	2.292e+00	-4.600e-06	6.703e-03	4671	6374	-0.78	0.39
58	0.035	360	5538.52	3.771e+01	3.565e-01	2.561e-02	1.713e+00	-4.423e-06	7.891e-03	4624	6403	-0.72	0.39
59	0.029	370	5546.51	2.280e+02	2.684e+01	-3.851e-02	8.539e-01	1.358e-06	3.512e-03	4730	6374	-0.84	0.35
60	0.025	384	5553.58	1.295e+02	2.011e+01	-7.179e-03	-2.188e+00	-1.418e-06	4.183e-03	4578	6361	-0.78	0.39
61	0.020	389	5560.22	-1.011e+02	-1.202e+00	7.554e-02	-3.020e+00	-8.479e-06	8.282e-03	4671	6374	-0.84	0.35
62	0.023	373	5587.58	-2.720e+02	-2.587e+01	1.295e-01	3.830e+00	-1.321e-05	1.214e-02	4624	6374	-0.78	0.39
63	0.024	397	5618.64	-9.415e+01	6.043e+00	7.345e-02	-3.181e+00	-8.369e-06	6.800e-03	4556	6374	-0.84	0.39
64	0.024	355	5619.60	1.379e+02	7.949e+01	-1.050e-02	1.627e+01	-1.276e-06	-5.066e-03	4556	6374	-0.56	0.39
65	0.023	381	5635.83	-5.765e+01	2.943e+01	5.610e-02	4.510e-01	-6.946e-06	2.472e-03	4578	6374	-0.70	0.39
66	0.019	242	5636.70	-2.439e+02	9.714e+00	1.189e-01	5.799e+00	-1.271e-05	4.970e-03	4556	6161	-0.43	0.39
67	0.012	132	5638.27	1.676e+02	5.739e+00	-5.661e-03	-9.538e-01	-1.721e-06	7.890e-03	4879	6374	-0.83	0.18
68	0.017	257	5641.44	-2.810e+01	3.885e+01	6.422e-02	5.051e-01	-8.293e-06	3.287e-03	4578	6374	-0.84	0.30
69	0.022	361	5649.99	-8.049e+00	6.051e+01	3.329e-02	1.014e+01	-4.440e-06	-2.451e-03	4785	6374	-0.60	0.39
70	0.019	216	5651.47	-7.249e+01	4.275e+01	5.219e-02	8.845e+00	-6.298e-06	-1.049e-03	4578	6161	-0.41	0.39
71	0.040	339	5652.32	-1.100e+01	9.628e+01	3.323e-02	2.182e+01	-4.610e-06	-1.017e-02	4556	6361	-0.62	0.39
72	0.026	272	5661.35	-3.620e+00	1.124e+02	3.146e-02	2.313e+01	-4.637e-06	-1.280e-02	4556	6287	-0.54	0.39
73	0.029	340	5667.52	-5.022e+01	3.480e+01	6.549e-02	8.794e+00	-8.263e-06	4.560e-03	4556	6374	-0.84	0.33
74	0.017	315	5679.03	1.396e+02	1.971e+01	-3.645e-03	-4.596e+00	-1.765e-06	5.075e-03	4749	6374	-0.84	0.33

Table 2. continued.

id	*stddev*	*ns*	λ	c_0	c_1	c_2	c_3	c_4	c_5	T_{eff}^{min}	T_{eff}^{max}	*fehmin*	*fehmax* †
75	0.017	181	5715.09	1.853e+02	2.684e+01	-7.341e-03	4.650e+00	-2.123e-06	5.455e-03	4649	6403	-0.83	0.21
76	0.016	350	5731.77	5.208e+01	7.093e+00	2.631e-02	-1.336e+00	-4.375e-06	7.272e-03	4649	6403	-0.84	0.33
77	0.025	123	5738.24	-1.048e+02	1.380e+02	6.458e-02	2.746e+01	-7.641e-06	-1.874e-02	4556	5914	-0.20	0.39
78	0.020	362	5741.85	-2.092e+01	4.235e+01	4.233e-02	6.322e+00	-5.725e-06	3.309e-04	4578	6361	-0.70	0.39
79	0.022	378	5752.04	-8.798e+01	-1.295e+01	7.141e-02	-2.124e+00	-8.080e-06	1.065e-02	4730	6374	-0.84	0.35
80	0.018	327	5775.08	-2.884e+01	-2.385e+00	5.526e-02	-2.220e+00	-6.923e-06	8.942e-03	4728	6374	-0.84	0.33
81	0.018	287	5778.46	1.890e+01	4.506e+01	3.776e-02	7.088e+00	-6.442e-06	-2.017e-04	4556	6161	-0.70	0.39
82	0.030	387	5793.92	5.060e+01	5.856e+01	1.629e-02	-2.570e-01	-3.303e-06	-3.114e-03	4649	6374	-0.72	0.39
83	0.031	371	5806.73	-2.200e+02	2.733e+01	1.206e-01	1.304e+00	-1.263e-05	4.599e-03	4578	6374	-0.84	0.34
84	0.032	356	5809.22	2.561e+02	1.174e+02	-3.839e-02	7.787e+00	4.498e-07	-1.101e-02	4578	6374	-0.84	0.35
85	0.014	271	5814.81	-5.541e+01	5.903e+01	4.968e-02	1.129e+01	-6.253e-06	-3.345e-03	4556	6227	-0.54	0.39
86	0.029	99	5827.88	2.484e+02	1.757e+02	-6.769e-02	2.119e+01	4.691e-06	-2.744e-02	4595	5886	-0.32	0.39
87	0.021	381	5852.22	5.740e+01	6.228e+01	1.907e-02	5.890e+00	-3.794e-06	-2.186e-03	4624	6403	-0.78	0.39
88	0.015	266	5855.08	-1.581e+02	4.554e+01	8.292e-02	1.032e+01	-8.931e-06	-1.120e-03	4578	6227	-0.38	0.39
89	0.017	386	5856.09	-1.141e+02	2.988e+01	7.359e-02	6.299e+00	-8.302e-06	2.511e-03	4624	6403	-0.70	0.39
90	0.035	95	5902.48	-2.580e+02	4.483e+01	1.138e-01	2.863e+01	-1.150e-05	-4.066e-03	4723	5914	-0.07	0.39
91	0.032	319	5916.26	1.395e+02	-8.026e+00	5.336e-03	-4.553e+00	-3.450e-06	9.420e-03	4649	6374	-0.84	0.33
92	0.030	383	5927.79	-8.166e+01	-7.428e+00	6.484e-02	-2.926e+00	-7.472e-06	9.326e-03	4578	6403	-0.78	0.39
93	0.033	393	5929.68	-6.996e+01	-5.744e-02	5.875e-02	-6.093e+00	-6.873e-06	7.402e-03	4649	6403	-0.78	0.39
94	0.022	136	5934.66	9.081e+01	-1.922e+01	2.423e-02	-4.132e+00	-4.644e-06	1.236e-02	5023	6374	-0.84	0.21
95	0.023	292	5956.70	1.979e+02	7.238e+00	-4.371e-03	3.304e+00	-3.624e-06	6.958e-03	4820	6403	-0.84	0.35
96	0.019	305	6027.06	-3.348e+01	-1.738e+01	5.513e-02	-1.116e+00	-6.600e-06	1.110e-02	4671	6374	-0.84	0.30
97	0.023	190	6056.01	-1.434e+02	-5.097e+01	9.439e-02	-3.554e+00	-9.882e-06	1.737e-02	4578	6374	-0.84	0.21
98	0.016	142	6078.49	2.758e+02	6.500e+01	-4.065e-02	3.100e+00	1.085e-06	-1.103e-03	4879	6374	-0.84	0.18
99	0.020	390	6079.01	-7.753e+01	3.215e+01	6.533e-02	9.778e-01	-7.603e-06	2.745e-03	4671	6403	-0.78	0.39
100	0.017	374	6082.72	1.050e+02	4.141e+01	1.286e-02	5.201e+00	-4.321e-06	7.475e-04	4624	6361	-0.84	0.39
101	0.033	375	6089.57	-4.388e+01	2.996e+01	5.058e-02	7.216e+00	-6.371e-06	2.512e-03	4556	6361	-0.72	0.39
102	0.020	220	6094.38	-3.242e+02	3.546e-01	1.431e-01	7.829e+00	-1.445e-05	7.125e-03	4556	6161	-0.28	0.39
103	0.017	375	6096.67	3.028e+01	6.386e+01	3.210e-02	3.028e+00	-5.310e-06	-2.434e-03	4671	6361	-0.70	0.39
104	0.026	165	6098.25	-1.722e+02	4.669e+01	8.482e-02	2.465e+01	-9.018e-06	-3.001e-03	4556	6161	-0.25	0.39
105	0.017	358	6151.62	8.572e+01	2.699e+00	2.460e-02	9.152e-01	-5.321e-06	7.643e-03	4578	6374	-0.84	0.35
106	0.031	325	6157.73	-6.641e+01	-2.480e+01	6.653e-02	-8.756e+00	-7.682e-06	1.155e-02	4578	6374	-0.84	0.35
107	0.036	389	6165.36	-1.978e+02	-3.319e+01	1.046e-01	-3.580e+00	-1.081e-05	1.340e-02	4556	6374	-0.84	0.39
108	0.015	192	6173.34	2.765e+02	2.456e+00	-3.815e-02	-1.829e+00	3.782e-07	7.731e-03	4879	6361	-0.83	0.30
109	0.016	369	6187.99	1.513e+02	6.428e+01	-4.207e-03	3.402e+00	-2.372e-06	-1.913e-03	4750	6403	-0.84	0.35
110	0.015	159	6200.32	2.515e+02	-1.202e+01	-2.843e-02	-2.718e+00	-4.263e-07	1.051e-02	4900	6361	-0.83	0.21
111	0.020	239	6220.79	9.946e+01	8.621e+01	-2.926e-03	1.944e+01	-1.916e-06	-8.336e-03	4556	6161	-0.56	0.39
112	0.018	336	6226.74	-4.656e+01	6.611e+01	5.308e-02	1.105e+01	-6.895e-06	-3.410e-03	4624	6276	-0.56	0.39
113	0.019	375	6229.24	-1.655e+00	6.564e+00	4.449e-02	5.706e+00	-6.467e-06	7.753e-03	4556	6374	-0.72	0.39
114	0.038	322	6238.39	-3.487e+02	-3.509e+01	1.158e-01	1.462e+01	-8.241e-06	1.371e-02	4831	6361	-0.67	0.39
115	0.016	360	6240.65	6.372e+01	3.407e+00	3.232e-02	1.895e+00	-6.022e-06	7.794e-03	4624	6403	-0.78	0.35
116	0.016	375	6270.23	2.415e+01	1.398e+01	4.272e-02	2.571e+00	-6.554e-06	5.993e-03	4624	6374	-0.84	0.35
117	0.028	391	6315.81	-1.179e+02	1.939e+01	7.977e-02	3.463e+00	-9.014e-06	4.853e-03	4578	6403	-0.70	0.35
118	0.017	140	6322.69	1.652e+02	-8.515e+00	1.986e-03	-3.437e+00	-3.022e-06	9.911e-03	5023	6374	-0.84	0.19
119	0.010	94	6358.68	1.589e+02	4.306e+01	3.146e-02	2.037e+00	-7.674e-06	4.734e-03	5417	6374	-0.78	0.21
120	0.036	397	6380.75	-2.942e+02	-2.097e+01	1.426e-01	-5.316e+00	-1.429e-05	1.144e-02	4556	6374	-0.84	0.35
121	0.018	240	6392.54	-1.515e+02	1.361e+01	9.765e-02	3.821e+00	-1.188e-05	4.910e-03	4578	5989	-0.72	0.39
122	0.024	233	6481.88	-2.832e+01	-4.473e+01	6.769e-02	2.801e-01	-8.946e-06	1.604e-02	4649	6403	-0.83	0.30
123	0.027	331	6498.94	2.621e+02	-2.801e+01	-3.054e-02	-7.395e+00	-1.192e-06	1.237e-02	4649	6374	-0.84	0.39
124	0.021	247	6608.03	-1.104e+02	3.988e+01	8.333e-02	5.617e+00	-1.062e-05	1.996e-04	4578	5989	-0.72	0.39
125	0.015	219	6609.12	1.566e+02	1.759e+01	4.808e-03	4.456e+00	-3.536e-06	6.485e-03	4649	6374	-0.84	0.30
126	0.023	229	6625.02	1.285e+02	6.232e+01	6.883e-03	8.233e+00	-4.658e-06	-3.701e-03	4556	5914	-0.72	0.39
127	0.018	326	6627.55	-1.703e+02	8.829e+01	9.358e-02	1.550e+01	-1.023e-05	-7.453e-03	4578	6260	-0.50	0.39
128	0.016	380	6703.57	2.267e+01	2.445e+01	3.990e-02	3.450e+00	-6.453e-06	4.010e-03	4556	6361	-0.78	0.39
129	0.018	390	6705.11	-8.592e+01	5.960e+01	7.263e-02	6.213e+00	-8.585e-06	-1.000e-03	4556	6361	-0.78	0.35
130	0.022	229	6710.32	7.043e+01	7.075e+01	2.311e-02	1.057e+01	-5.682e-06	-4.916e-03	4556	5917	-0.72	0.39
131	0.021	292	6713.05	-2.097e+02	6.184e+01	1.048e-01	9.106e+00	-1.111e-05	-3.766e-03	4671	6161	-0.41	0.39
132	0.017	236	6713.74	-2.250e+02	3.797e+01	1.056e-01	1.325e+01	-1.090e-05	-3.997e-05	4647	6161	-0.32	0.39
133	0.019	193	6725.36	-2.724e+02	3.980e+01	1.287e-01	7.781e+00	-1.362e-05	9.816e-05	4698	5989	-0.26	0.39
134	0.020	382	6726.67	-1.289e+01	4.785e+01	4.599e-02	2.696e+00	-6.151e-06	5.169e-04	4671	6403	-0.78	0.39
135	0.017	311	6733.15	-2.182e+02	4.476e+01	1.088e-01	7.913e+00	-1.148e-05	2.804e-05	4624	6227	-0.45	0.39
136	0.019	172	6739.52	2.370e+01	6.136e+01	3.417e-02	9.389e+00	-6.356e-06	-4.288e-03	4556	5827	-0.72	0.39
137	0.021	306	6786.86	-1.150e+02	5.132e+01	7.364e-02	8.126e+00	-8.511e-06	-1.370e-03	4556	6276	-0.54	0.39
138	0.024	110	6793.26	4.719e+01	2.173e+02	5.951e-04	5.214e+01	-1.032e-06	-3.675e-02	4647	5914	-0.20	0.39
139	0.027	359	6806.85	-4.387e+01	4.316e+01	6.488e-02	4.865e+00	-8.845e-06	9.710e-04	4556	6361	-0.78	0.35
140	0.021	376	6810.27	-4.150e+01	3.646e+01	5.659e-02	1.603e+00	-7.038e-06	2.640e-03	4595	6374	-0.84	0.35
141	0.016	377	6820.37	-2.306e+01	5.392e+01	4.775e-02	7.352e+00	-6.336e-06	-3.263e-04	4649	6374	-0.78	0.35
142	0.027	367	6828.60	-1.282e+02	1.418e+01	8.794e-02	1.754e+00	-9.707e-06	6.572e-03	4556	6403	-0.84	0.33
143	0.024	174	6837.01	-1.395e+02	3.806e+01	7.098e-02	1.724e+01	-7.564e-06	-1.265e-03	4556	6161	-0.22	0.39
144	0.028	345	6839.84	2.072e+02	1.071e+02	-2.714e-02	1.279e+01	-5.973e-07	-1.090e-02	4556	6287	-0.78	0.39
145	0.019	384	6842.69	-7.707e+01	6.390e+01	6.450e-02	2.873e+00	-7.684e-06	-2.778e-03	4671	6289	-0.70	0.35
146	0.025	328	6843.66	-2.222e+02	3.112e-01	1.244e-01	-1.969e+00	-1.305e-05	9.038e-03	4595	6374	-0.84	0.33
147	0.033	205	6855.72	1.443e+02	2.005e+02	-3.124e-02	5.407e+01	1.691e-06	-3.082e-02	4595	6161	-0.25	0.39
148	0.017	272	6857.25	-1.797e+02	1.675e+01	9.315e-02	8.259e+00	-1.005e-05	4.228e-03	4556	6227	-0.52	0.39
149	0.028	379	6858.15	-1.407e+02	6.900e+00	9.054e-02	-6.242e-01	-9.878e-06	7.621e-03	4556	6374	-0.84	0.35

Table 2. continued.

id	*stddev*	*ns*	λ	c_0	c_1	c_2	c_3	c_4	c_5	T_{eff}^{min}	T_{eff}^{max}	*fehmin*	*fehmax* †
150	0.025	244	6861.94	2.667e+02	9.333e+01	-5.126e-02	2.030e+01	1.418e-06	-8.969e-03	4578	6026	-0.72	0.39
151	0.026	340	6862.50	-2.833e+02	2.371e+01	1.330e-01	7.602e+00	-1.359e-05	3.926e-03	4556	6361	-0.54	0.39

† The columns correspond to the following: *id* is the ID number of the line; *ns* is the number of stars used for line calibration (out of a total of 451); *stddev* is the final standard deviation for each calibration; λ is the wavelength of the calibrated line; c_0, c_1, c_2, c_3, c_4, and c_5 are the fitting coefficients for each line; T_{eff}^{min} and T_{eff}^{max} are the limits in effective temperature of the stars used to calibrate each line; *fehmin* and *fehmax* are the limits in [Fe/H] of the stars used to calibrate each line.